Frequency-Division-Multiplexed Signal and Power Transfer for Wearable Devices Networked via Conductive Embroideries on a Cloth

Akihito Noda and Hiroyuki Shinoda
The University of Tokyo, Kashiwa-shi, Chiba 277-8561, Japan

***Abstract*—We propose a powering scheme for tiny wearable devices attached on a cloth without individual one-to-one wires. Devices with a special connector consisting of a tack and a clutch are stuck through a special cloth embroidered with conductive threads. Physical mounting of the devices and electrical connection are integrated into a single action, i.e., just sticking the connector. Combining microwave/high-frequency circuit technology and recent highly conductive soft fabric materials opens up a new implementation scheme for wearable sensing/display/communication systems.**

***Index Terms*—Conductive embroidery, e-textiles, wearable networks.**

I. Introduction

Smart fabrics, or e-textiles, that support sensing and/or actuating capabilities on a user's body surface while eliminating the use of a number of individual wires is one of the key technologies for wearable systems [1]. Such a technology will enable new implementation schemes for biomonitoring [2], [3], embodied user interfaces [4], etc.

Wireless technologies, including wireless power transfer (WPT) [5], have seen a dramatic evolution in the past decades. In the context of smart fabrics, wearable fabric antennas for communication [6] and energy harvesting [7] have attracted considerable attention. However, wireless schemes inherently suffer from interference; therefore, nonwireless, electric-contact-based schemes still have advantages for some applications.

For providing such contact-based connections in wearable systems, circuit patterning on a fabric with conductive threads [8] and conductive screen printing ink [9], instead of copper patterns used on conventional printed circuit boards (PCBs), is one of the most straightforward and practical approaches. This approach requires separated conductive lines individually connecting leads/pins of electronic components, as in conventional PCBs. A possible vulnerability is that fraying/whiskering the fabric would cause a fatal breakdown, such as a short circuit between neighboring conductive lines or disconnection of lines.

To eliminate one-to-one wiring, conductive-fabric-based approaches have been proposed [10], [11]. These schemes require at least triple-layered fabrics: the top and the bottom conductor layers, and an insulator layer between them. The two conductive fabric sheets work as a signal bus line shared by all devices mounted on the fabric. TextileNet proposed by Akita et al. enables dc power supply and serial communication on the bus, by temporally switching the power supply state and the pulse transfer state [11]; thus, the power supply is intermittent and only singleplex signal transfer is supported.

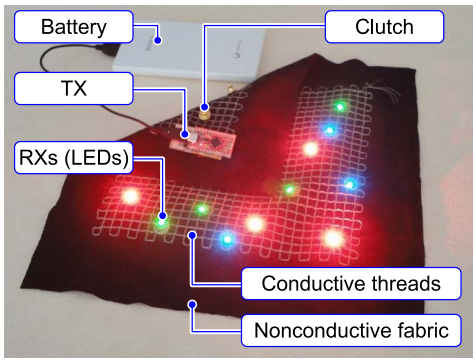

(a)

(b)

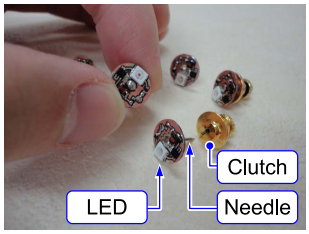

(c)

Fig. 1: (a) A wearable signal/power transfer cloth and receiver (RX) devices. The top left-hand side of the sheet is folded and the bottom surface is shown. A transmitter (TX) is attached on the bottom side. (b) Each channel can be selectively turned on. Only one channel (red LEDs) is turned on in this figure. The sheet retains stretchability of the original base fabric in a direction biased to the embroidered conductive threads. (c) Fabricated RXs, each loaded with an LED.

In this paper, we propose another scheme using a similar fabric-based material and tack connectors as shown in Fig. 1. An arbitrary nonconductive fabric sheet can be used as the base fabric, and conductive threads are sewn on both the sides of the base fabric. Let this material be referred to as the conductive-thread-embroidered fabric (CTEF). The conductive threads on opposite sides are isolated from each other; thus, the CTEF works in almost the same manner as the above-mentioned triple-layered fabrics. The advantages of our proposal are as follows: 1) the CTEF can in part retain the thinness, flexibility, stretchability, and texture of the original base fabric; 2) frequency-division-multiplexing (FDM) enables multichannel on-off control of receiver (RX) devices whereas the dc power is continuously supplied; and 3) the capability of on-off keying (OOK) of each channel enables

978-1-5090-6360-4/17/$31.00 ©2017 IEEE

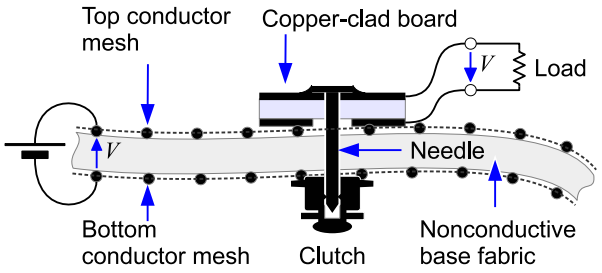

Fig. 2: Cross-sectional view of a wearable signal/power transfer sheet and a tack connector. Although the mesh conductors are represented with separate dots (and a dotted line connecting them) in this figure, each of them is electrically continuous. The top and the bottom mesh conductors are isolated from each other.

pulse-width modulation (PWM) and provides potential to be combined with other serial communication protocols such as Inter-Integrated Circuit (I^2C) [12]. Although a primitive idea of an FDM-based scheme has been presented in our previous work [13], the practical implementation of the scheme has not been reported. This paper presents a wearable demonstration system with practical TX/RX circuits.

In the rest of the paper, we describe a CTEF and a tack connector, show an example of the FDM implementation, present an actually wearable demonstration system, and draw our conclusions.

II. Conductive Embroideries and Tack Connectors

A cross-section of the proposed structure of a CTEF and a tack connector is illustrated in Fig. 2. Conductive threads are sewn onto each side of a nonconductive base fabric. Although the conductive threads are arranged in a square mesh pattern in this work, as shown in Fig. 1, they can be arbitrarily arranged in any other geometric patterns and any other artwork patterns.

An essential requirement is that the conductive meshes on both the sides are electrically isolated from each other. This is achieved by sewing the conductive threads onto each side with another nonconductive thread. The conductive threads do not pierce the nonconductive base fabric.

As shown in Fig. 2, a special connector consisting of a tack (needle) and a clutch is used in this work. The needle is stuck through the CTEF from one side and the clutch is attached on the other side. The needle should avoid piercing the thread of top conductor mesh, to avoid short circuit between the top and the bottom conductor threads via the needle.

This configuration allows the physical mounting of a device and its electrical connection to be integrated into a single action, i.e., just sticking the connector.

III. Frequency-Division Multiplexing

To achieve independent multichannel on-off control of the power supply on a CTEF, an FDM-based scheme is implemented in the system, as shown in Fig. 3.

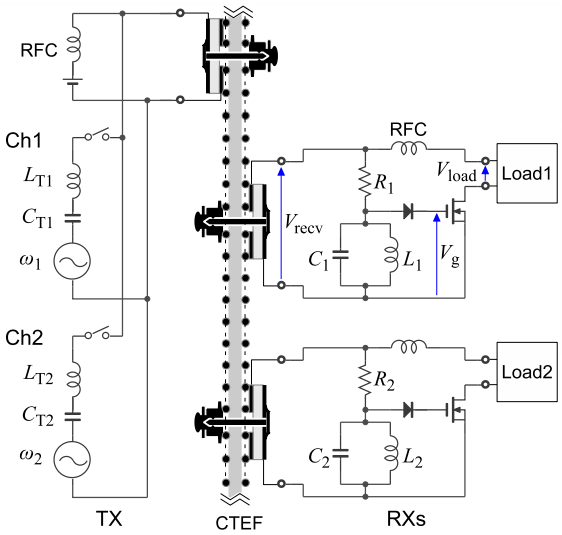

Fig. 3: A multiplexed power transfer system on a single CTEF.

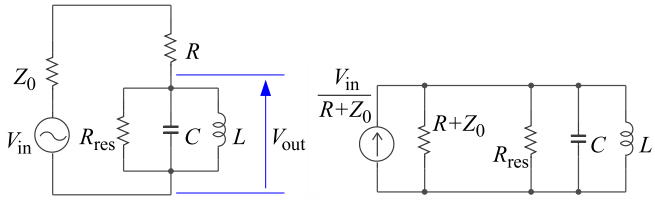

Fig. 4: (a) RF equivalent circuit of a receiver filter. (b) Norton's equivalent circuit of (a).

A. Receiver Circuit

A parallel LC tank with a series resistor is embedded in each RX. Signals picked up from the CTEF are applied to this RLC network. The voltage appearing across the LC tank is rectified and is fed to the gate of an output FET.

The FET is turned on by the signal at the fixed resonant frequency of the LC tank. By choosing the values of L and C appropriately, each RX can be configured to have sensitivity to a signal of a particular frequency.

An equivalent circuit model of the RLC filter is shown in Fig. 4(a), and it is expressed as Fig. 4(b), according to Norton's theorem. The voltage gain G at the resonant frequency and the quality factor Q of the RLC network are respectively expressed as follows:

$$G = \frac{V_{\text{out}}}{V_{\text{in}}} = \frac{R_{\text{res}}}{(Z_0 + R) + R_{\text{res}}} \quad (1)$$

$$Q = \frac{\omega C}{(Z_0 + R)^{-1} + R_{\text{res}}^{-1}} = \frac{1}{\omega L\{(Z_0 + R)^{-1} + R_{\text{res}}^{-1}\}}, \quad (2)$$

where ω_0 and Z_0 denote the resonant frequency and the source impedance seen looking from the RX, respectively. R_{res} represents the equivalent parallel resistance of the LC tank, which determines its unloaded quality factor. As shown in the above equations, the voltage gain, which determines the sensitivity of the RX, decreases with increasing series

978-1-5090-6360-4/17/$31.00 ©2017 IEEE

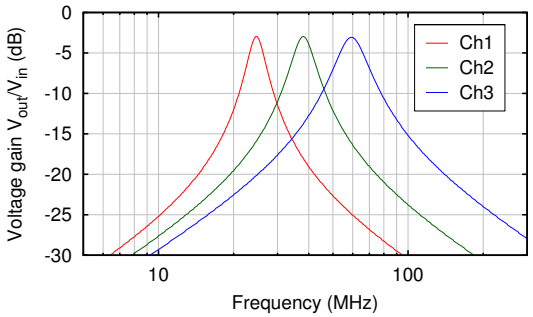

Fig. 5: Simulated voltage gain of the designed RLC filters.

resistance R; and the quality factor, i.e., the selectivity of the filter, increases with increasing R. Thus, the sensitivity and selectivity are in trade-off.

Simulated voltage gains of the RLC networks, designed for three channels at 25 MHz, 40 MHz, and 54 MHz, are shown in Fig. 5. These results were obtained by using LTspice [14]. The SPICE simulation parameters are shown in Table I. Note that parasitic components were also included in the simulation by using SPICE models provided by the manufacturer of the inductors [15]. Since the capacitors were less lossy compared with the inductors, the capacitors were approximated with ideal capacitors in the simulation. The gain of each filter provides an attenuation more than 10 dB at the frequency of other channels, compared with the peak gain.

B. Transmitter Circuit and Frequency Assignment

The transmitter circuit consists of the dc and multiple high-frequency (HF) signal sources, as shown in Fig. 3. The HF sources are connected to the bus via a series LC tank circuit. The LC tanks and the choke inductor (RFC) prevent excess current flowing among the dc and HF sources because of the direct connection.

An example implementation of the TX circuit is shown in Fig. 6. A one-chip multichannel clock signal generator Si5351A from Silicon Laboratories Inc., and FET amplifiers were used as multiple HF signal sources. The clock generator was controlled by a microcontroller unit (MCU) Pro Micro from SparkFun Electronics. The MCU board was powered by a 5-V portable charger via its USB Micro-B interface. A 3.3-V dc voltage was supplied from the MCU board to a CTEF as well as the HF signals from the clock generator. Thus, the 3.3-V dc voltage and HF signals were superposed on the bus, i.e., the conductive embroideries on both sides.

Examples of voltage waveforms measured on RXs are shown in Fig. 7. V_{recv}, V_{g}, and V_{load} respectively correspond to the same symbols indicated in Fig. 3. Each RX was loaded

TABLE I
CIRCUIT PARAMETERS IN SPICE SIMULATION

	R (kΩ)	L (μH)	C (pF)	Z_0 (Ω)
Channel 1	4.7	3.3	12	0
Channel 2	5.6	3.3	5	0
Channel 3	6.5	3.3	2	0

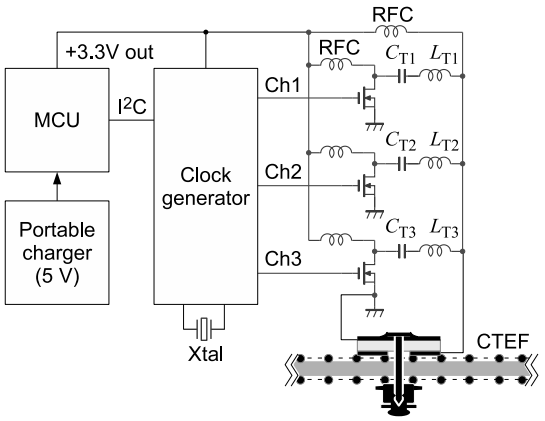

Fig. 6: Schematic diagram of a TX circuit. The MCU controls the frequency and the on/off state of each output channel of the clock generator.

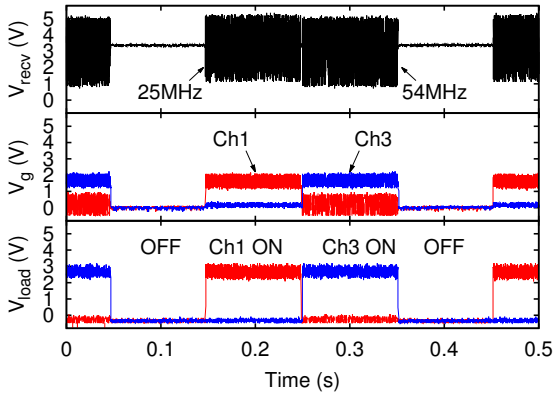

Fig. 7: Waveforms measured on two receivers, corresponding to channels 1 and 3. Both of them receive the same signal, shown as V_{recv}. The gate voltage V_{g} rises when the HF signal corresponding to the resonant frequency of the LC tank is received. Then, the FET is turned on and a dc voltage, approximately 2.7 V, is supplied to the load.

with a 30-Ω resistor. The FET is turned on and a dc voltage is supplied to the load, when the HF signal corresponding to the resonant frequency of the LC tank is received.

Channel frequency assignment in the proposed scheme depends on the size of the CTEF, termination of the CTEF, requirements of power-on/off switching frequency, and Q of RX. In this paper, we assume that the CTEF is approximately 50-cm square and is not terminated with resistors or radio wave absorbers. In an unterminated CTEF, the wavelength of the electromagnetic wave should be significantly larger than the size of the CTEF. Otherwise, the received voltage amplitude will vary depending on the RX position, because of the standing waves generated in the CTEF. The acceptable range of the received signal strength depends on the dynamic range of the HF detection circuit in RXs. Hence, for a 50-cm square CTEF, the signal frequency should be lower than 60 MHz, which corresponds to a 5-m wavelength, to prevent

978-1-5090-6360-4/17/$31.00 ©2017 IEEE

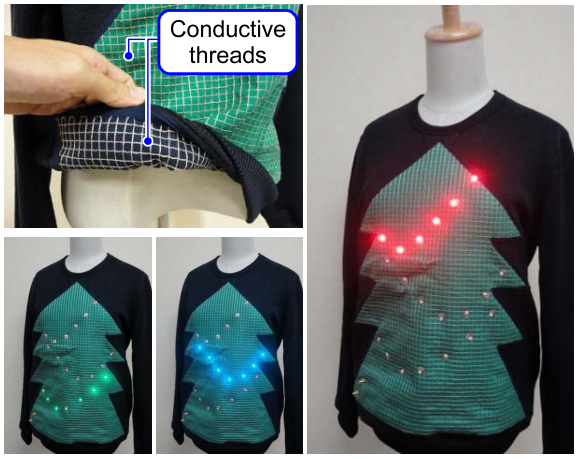

Fig. 8: A wearable demonstration system. Single-sided CTEF patches are sewn on both of the inside and the outside surfaces of clothing (top left). Three channels (green, blue, and red LEDs) can be independently turned on and off (bottom left, bottom middle, right).

significant signal strength variance. On the other hand, the lower bound of the carrier frequency range depends on the frequency of modulation, i.e., the on-off frequency of the power supply connected to the load. Based on these requirements, we determined the channel frequencies as 25 MHz, 40 MHz, and 54 MHz. These were determined as just an example and were not optimized; nevertheless, the system works well as shown by Figs. 1 and 8.

IV. Demonstration System

An actual wearable demonstration system is shown in Fig. 8. This signal/power-transferring wear was fabricated by sewing single-sided CTEF patches on both the inside and the outside of commercially available clothing. Thus, the signal/power transfer functionality is retrofittable to off-the-shelf clothing.

Each RX is loaded with an LED. The LEDs for the RX loads were chosen to visually demonstrate satisfactory system operation. More power-consuming RX loads, such as vibrators and other actuators typically used for providing tactile feedback to users, can be driven with this system.

The resistance of the conductive mesh was less than 1.5 Ω between any two points on a 180-mm square mesh-embroidery shown in Fig. 1. Thus, the equivalent resistance connected in series between the TX and an RX is less than 3.0 Ω. For a 10-Ω load, which is the minimum load resistance that can be driven with a USB 2.0 interface, the power transmission efficiency, defined as the ratio of the power consumed at the load to the sum of the power consumed at the load and that consumed at the 3.0-Ω equivalent resistance, will be 77%. One of the potential applications of the demonstrated system is in a wearable tactile display suit with densely distributed tactile actuators that can be controlled independently. Eliminating one-to-one wiring to each of these actuators will provide significant advantages for such a wearable system.

V. Conclusion

We proposed a power supply scheme with a capability of multiplexed on-off control via a fabric sheet embroidered with conductive threads without one-to-one harness. Arbitrary clothing can be used as a signal/power-transferring medium for wearable systems, by adding conductive embroideries while retaining in part the flexibility and stretchability of the original cloth. The FDM-based scheme achieved simultaneous multi-channel on-off control with a continuous dc power supply. The OOK-based communication schemes including PWM control and serial communication protocols can be implemented on the multiplexed on-off channels. The proposed scheme combining high-frequency circuit technologies and emerging soft conductive material technologies will provide a new paradigm for wearable network implementations.

Acknowledgment

This work was supported in part by the JST ACCEL Embodied Media Project and the MIC/SCOPE #155103003. We thank Mr. Yoshiaki Hirano and Ms. Junko Yamada, Teijin Limited, for providing the CTEF materials.

References

[1] M. Stoppa and A. Chiolerio, "Wearable electronics and smart textiles: A critical review," *Sensors*, vol. 14, no. 7, pp. 11 957–11 992, 2014.
[2] S. Patel, H. Park, P. Bonato, L. Chan, and M. Rodgers, "A review of wearable sensors and systems with application in rehabilitation," *Journal of NeuroEngineering and Rehabilitation*, vol. 9, no. 1, pp. 1–17, 2012.
[3] A. Shafti, R. B. R. Manero, A. M. Borg, K. Althoefer, and M. J. Howard, "Designing embroidered electrodes for wearable surface electromyography," in *IEEE ICRA 2016*, May 2016, pp. 172–177.
[4] K. P. Fishkin, T. P. Moran, and B. L. Harrison, "Embodied user interfaces: Towards invisible user interfaces," in *Engineering for Human-Computer Interaction*. Springer, 1999, pp. 1–18.
[5] N. Shinohara, "Power without wires," *IEEE Microwave Magazine*, vol. 12, no. 7, pp. S64–S73, December 2011.
[6] N. H. M. Rais, P. J. Soh, F. Malek, S. Ahmad, N. B. M. Hashim, and P. S. Hall, "A review of wearable antenna," in *2009 Loughborough Antennas Propagation Conference*, Nov 2009, pp. 225–228.
[7] S. Lemey, F. Declercq, and H. Rogier, "Textile antennas as hybrid energy-harvesting platforms," *Proceedings of the IEEE*, vol. 102, no. 11, pp. 1833–1857, Nov 2014.
[8] L. Buechley and M. Eisenberg, "The LilyPad Arduino: Toward Wearable Engineering for Everyone," *IEEE Pervasive Computing*, vol. 7, no. 2, pp. 12–15, Apr. 2008.
[9] Y. Kim, H. Kim, and H. J. Yoo, "Electrical characterization of screen-printed circuits on the fabric," *IEEE Transactions on Advanced Packaging*, vol. 33, no. 1, pp. 196–205, Feb 2010.
[10] E. Wade and H. H. Asada, "Cable-free wearable sensor system using a DC powerline body network in a conductive fabric vest," in *IEEE EMBC 2004*, vol. 2, Sept. 2004, pp. 5376–5379.
[11] J. Akita, T. Shinmura, and M. Toda, "Flexible network infrastructure for wearable computing using conductive fabric and its evaluation," in *IEEE ICDCSW'06*, Jul., 2006, p. 65.
[12] N. Semiconductors, "UM10204: I2C-bus specification and user manual, Rev. 6," p. 11, 2014.
[13] Y. Tajima, A. Noda, and H. Shinoda, "Signal and power transfer to actuators distributed on conductive fabric sheet for wearable tactile display," in *Proc. of AsiaHaptics 2016*, Kashiwanoha, Japan, November 2016, pp. 1–6.
[14] Linear Technology. LTspice. [Online]. Available: http://www.linear-tech.co.jp/designtools/software/#LTspice
[15] TDK EPCOS Design Tools. [Online]. Available: https://en.tdk.eu/tdk-en/180514/design-support/design-tools/inductors

978-1-5090-6360-4/17/$31.00 ©2017 IEEE